EXPERIMENTAL INVESTIGATION OF THE EFFECT OF WAVE TURBULATORS ON HEAT TRANSFER IN PIPES

by

Sendogan KARAGOZ[a], Semih ERZINCANLI[a], Orhan YILDIRIM[a], Ilker FIRAT[b*], Mehmet KAYA[c], Omer COMAKLI[a], and Gokhan OMEROGLU[a]

[a] Department of Mechanical Engineering, Ataturk University, Erzurum, Turkey
[b] Ilic Dursun Yildirim Vocational School, Erzincan Binali Yildirim University, Erzincan, Turkey
[c] Department of Airframe and Powerplant Maintenance, Kocaeli University, Kocaeli, Turkey

Original scientific paper
https://doi.org/10.2298/TSCI210206183K

This experimental study deals with the heat transfer and friction effects of sinusoidal part turbulators for single-phase flows occurring in a circular shaped pipe. Turbulators with three different radius values are placed in the pipe to make the flow turbulent. In this way, changes in Nusselt number and friction coefficient are examined. As a result of the experiments made with Reynolds numbers in the range of 6614-20710, the increase rates of the Nusselt numbers of turbulators with 20 mm, 110 mm, and 220 mm radius compared to the empty pipe were obtained as 153.49%, 85.36%, and 52.09%, respectively. As a result of the decrease in the radius, there was an increase in the Nusselt number and the friction factor. Parallel to the Nusselt number, the highest friction factor was obtained in the smallest radius turbulator. It was found that the thermal enhancement factors of 110 mm and 220 mm radius turbulators increased by 179.54% and 132.95%, respectively, compared to the 20 mm radius turbulator. Similarly, it was determined that the thermal enhancement factor of the 110 mm radius turbulator increased by 20% compared to the 220 mm radius turbulator.

Key words: *turbulator, heat transfer, friction factor, press drop, turbulent flow*

Introduction

The supply of energy to the users as sufficient, timely, high quality, economical, reliable and clean is one of the most important indicators that determine the development levels of the countries. As the demand for energy, which is one of the most important inputs of the daily life of the public as well as the industry, is constantly increasing, the energy resources are rapidly depleting. To achieve a sustainable balance, it has gained great importance to provide energy resources diversity and to offer RES besides conventional energy sources. In today's world, where efficient and rational use of resources is subject to some disciplines, the importance of rational use of energy, which is the driving force of industry, transportation and our social life, also arises spontaneously.

Today, heat exchangers are widely used in different industries [1]. Extensive applications of heat exchangers including air conditioning, refrigeration, power plants, refineries, food industry, medicines, *etc.* have led to many studies to improve their productivity and performance in industry and society [2-6]. For this reason, it is necessary to use methods that can

* Corresponding author, e-mail: ifirat@erzincan.edu.tr

increase the efficiency of these heat exchangers to reach the main goal. In general, heat transfer techniques can be divided into three categories as active techniques, passive techniques or a combination of both [1]. Active techniques involve distortion of fluid flow using an external force such as magnetic fields [7] and pulsating flow [8]. In contrast, passive techniques require no external force and use solid particles [9], geometry modification [10] and vortex flow elements. Compound techniques use a combination of both techniques. Passive techniques are generally preferred because of their convenience, low cost, and pressure drop improvement properties [11].

Placing devices such as twisted tapes, wire springs, ribs, winglets, baffles *etc.* into the flow passage to generate vortex to increase the convective heat transfer rate is the most known processes in many thermal systems. In general, the purpose of increasing heat transfer is to reduce the pumping power for the heat transfer goal that saves operating costs or to make the heat exchangers more compact to reduce the overall dimensions and possibly costs of the heat exchangers [12]. For this reason, many studies have been performed to examine the effects of turbulators on increasing heat transfer.

Yaningsih *et al.* [13] experimentally examined the effect of the slant angle of the turbulators they used on single-phase forced convection heat transfer and internal flow friction factor. They made experimental comparisons between the conditions of the empty pipe and pipes with turbulators with slant angles of 15º, 20º and 25º, respectively, in the Reynolds number, ranging from 5300 to 17500. In their study, they stated that the heat transfer element provided 77.02% increase in heat transfer and 3.35 times more increase in friction factor compared to the empty pipe. Yakut and Sahin [14] investigated the effect of conical turbulators on heat transfer, pressure drop and flow-induced vibrations in turbulent flow. Anvari *et al.* [15] reported the effect of the conical turbulator on heat transfer using water as a test liquid. Promvonge and Eiamsa-ard [16] investigated the effect of heat transfer on the combined conical ring and twisted tape for twist ratios ranging from 3.75 to 7.5. Bhattacharyya *et al.* [17] investigated experimentally and numerically the heat transfer and fluid-flow properties of turbulent flow from a heat exchanger mounted with a circular twisted pipe. Kapse *et al.* [18] experimentally studied the heat transfer and pressure drop properties of three different passive crops for individual and compound addition. The experiments were carried out in a concentric circular tube in a tube heat exchanger, with water as the working fluid, in the range of 8000 to 32000 Reynolds number. As a result, they found the increase in Nusselt number and friction factors between 38-234% and 55-524%, respectively, compared to straight pipe. Sahel *et al.* [19] proposed the graded baffle-design for the friction factor that posed a problem for heat exchanger designers. Menni *et al.* [20] aimed to simulate oil flow characteristics in different geometric channels under turbulent regimes and forced-convection conditions. Ameur *et al.* [21] conducted numerical investigation on the performance of circular and elliptical perforated baffles in a plate-fin heat exchanger. As a result, they obtained thermal performance factors of 1.55 and 1.74 for circular and elliptical perforations, respectively.

In this experimental study, the effects of new types of turbulators manufactured in sinusoidal form with three different radii (20 mm, 110 mm, and 220 mm) on heat transfer and pressure drop for single phase flows occurring in a plain pipe were investigated.

Material and method

Experimental system

The aim of this experimental study is to determine which of the turbulators produced in various wavelengths has higher efficiency in terms of heat transfer. In addition, the aim is to examine whether these turbulators are more advantageous than other turbulators in the literature in terms of heat transfer.

Pure water was chosen as the test fluid in the experiments carried out in the Mechanical Engineering Department laboratory of Ataturk University. Schematic representation of the experimental system is given in fig. 1. The length, L, of the test pipe is 1.02 m and its inner diameter, D_i, is 0.0135 m. The length of the inlet section is 0.36 m, which is sufficient for turbulent flow to reach the hydrodynamically developed profile before entering the test section. Twelve equally spaced thermocouples are attached to the test part to measure the surface temperature. Two thermocouples are placed at the inlet and outlet of the test pipe to measure the temperature of the test liquid.

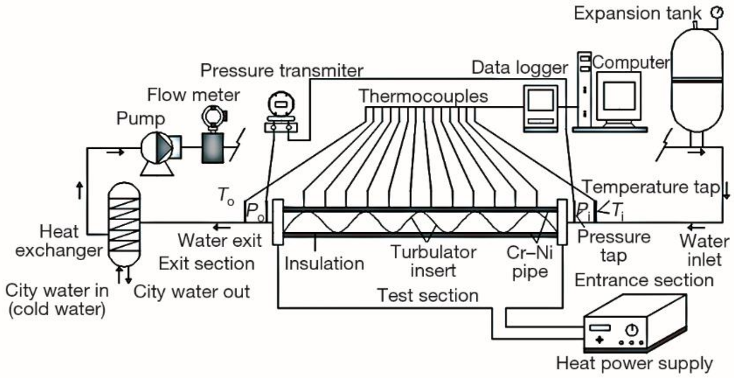

Figure 1. Schematic representation of the experimental system

All thermocouples are connected to a data logger for temperature recording:

- In the experimental set-up, a steel pipe made of Cr-Ni (stainless steel 316L) material with a length of 1020 mm and a diameter of 13.5 mm was used as a test tube.
- An expansion tank following the relevant standards was used to balance pressure losses and increases.
- A flow meter was used to measure the flow rate of the fluid used in the system.
- A circulation pump was used for the circulation of the test fluid used in the system.
- A power supply was used to provide the thermal energy needed in the system.
- A heat exchanger was used to bring the fluid entering the test tube to the desired temperature.
- Thermocouples were used to make measurements over the test tube.
- Pressure gauges were installed at the inlet and outlet of the test tube to measure pressure differences.
- The data in the experimental set-up were obtained with the data reading system.

In this study, temperatures, flow rates, pressure drops, voltages and currents were measured with the appropriate devices described:

- Measurement of the flow rate of the working fluid by a digital flow meter with a speed display.
- Measurement of the surface temperature with Cu-constantan thermocouples mounted on the outer surface of the test pipe in an equally spaced way.
- Measuring the inlet and outlet working fluid temperature with Cu-constantan thermocouples.
- Measurement of the pressure difference of the experimental unit with the pressure gauge placed at the inlet and outlet parts of the test section.
- Taking current and voltage values from the digital displays on the power source for the temperature needed by the test pipe.

The experimental set-up was filled with test fluid by taking the air of the system. Then, the system was started and waited until it became stable. When the system became stable, the data was taken digitally with the help of the advantec data reading device. This process was repeated in different flow rates of the fluid.

The *T*-type Cu-constantan temperature sensors were used to make temperature measurements in the experimental system. The attachment of thermocouples to the test pipe is given in fig. 2.

Figure 3 shows the attachment of thermocouples and insulation material to the test pipe schematically. Measurements were carried out by placing a total of 14 thermocouples, equally spaced 12 thermocouples on the outer surface of the test pipe (six on the lower surface, six on the upper surface) and two on the axis of the pipe to measure the inlet and outlet temperature of the fluid in the test zone. The data obtained from thermocouples were evaluated digitally by means of the advantec data reading device. The flow rate of the fluid at the inlet of the system and the static pressures at the inlet and outlet are other measured parameters.

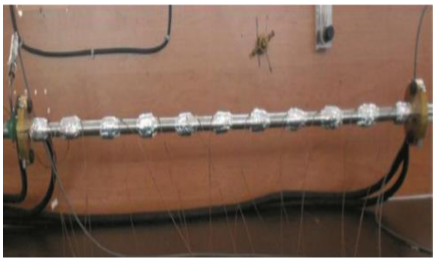

Figure 2. Attachment of thermocouples to the test pipe

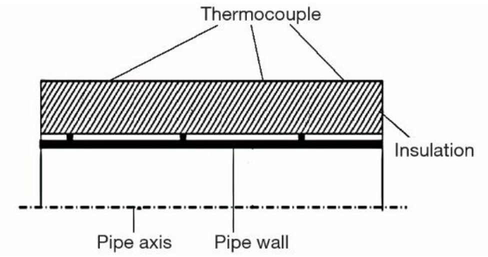

Figure 3. Schematic representation of the test pipe insulation layer and thermoelement ends

In the experimental set-up prepared, measurements were made with three turbulators with different radius values at three different flow rates. These measurements were compared with those made with the empty pipe.

For the turbulator radii of R = 20 mm, 110 mm, and 220 mm, measurements were made at 0.201, 0.301, and 0.401 m^3 per hours flow rates, respectively. The schematic representation of the turbulator radii is given in fig. 4. Turbulator strips were cut in accordance with the radius values determined on the CNC bench.

Wooden forms designed according to the radius values were used to make the turbulators strips twisted in a suitable way. The picture of wooden forms is given in fig. 5. Twisted turbulators were painted with spray paint to prevent electricity from the test pipe before placed inside the pipe. The picture of twisted turbulators is given in fig. 6.

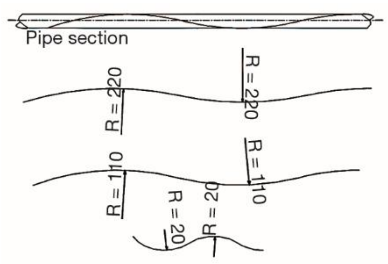

Figure 4. Turbulator radii

Figure 5. Wooden forms

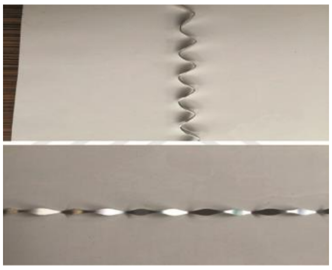

Figure 6. Twisted turbulators

The thermodynamic properties of the experimental system and the dimensions of the test pipe are given in tab. 1.

After the turbulators were placed in the pipe, the measurement phase was started. The view of the turbulator inside the pipe is given in fig. 7.

Table 1. Values of the experimental system

System pressure	100 kPa
Coolant flow rate	0.8 gallons per minute
Power supply capacity	500 W

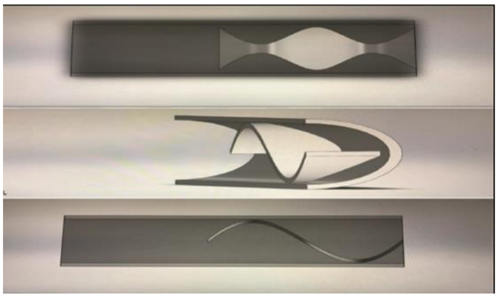

Figure 7. The view of the turbulator inside the pipe

Data reduction

The aim of this experiment is to examine the heat transfer, pressure drop and friction loss behavior of a circular pipe equipped with sinusoidal parts.

In this study, the test fluid, pure water flows through a pipe with uniform heat flux. Therefore, heat transfer is assumed to occur by convection and is expressed as in the following equation [22].

$$Q_{\mathrm{w}} = Q_{\mathrm{conv}} \tag{1}$$

$$Q_{\mathrm{w}} = mC_{p,\mathrm{w}}(T_{\mathrm{o}} - T_{\mathrm{i}}) \tag{2}$$

where Q_{w} [W] is the heat transfer to the pipe wall, Q_{conv} [W] – the heat transfer by convection, m [kg] – the mass, $C_{p,\mathrm{w}}$ [kJkg^{-1}K^{-1}] – the specific heat at constant pressure, and T_{i} [K] and T_{o} [K] – the inlet and outlet temperatures, respectively. The heat transfer of the pipe by convection is:

$$Q_{\mathrm{conv}} = hA(\overline{T}_{\mathrm{w}} - T_{\mathrm{b}}) \tag{3}$$

$$T_{\mathrm{b}} = \frac{T_{\mathrm{i}} + T_{\mathrm{o}}}{2} \tag{4}$$

$$A_y = \pi D_{\mathrm{i}} L \tag{5}$$

where the bulk temperature is shown as T_{b} [K] and the surface area as A_y [m^2]. The pipe inside diameter is expressed as D_{i} [m], and the length as L [m]:

$$\bar{T}_\mathrm{w} = \sum \frac{T_\mathrm{w}}{12} \tag{6}$$

where T_w [K] is the local surface temperature on the outer wall surface of the Cr-Ni pipe. The average wall temperature, $\bar{T}_\mathrm{w}$, is evaluated by taking the average of the local surface temperatures of 12 points equally spaced from the inlet to the outlet of the pipe.

$$D_\mathrm{h} = \frac{4A_\mathrm{c}}{D} = \frac{\frac{4\pi D_\mathrm{i}^2}{4}}{\pi D_\mathrm{i}} = D_\mathrm{i} \tag{7}$$

$$h = \frac{mC_{p,\mathrm{w}}(T_\mathrm{o} - T_\mathrm{i})}{A(\bar{T}_\mathrm{w} - T_\mathrm{b})} \tag{8}$$

$$\mathrm{Nu} = \frac{hD_\mathrm{i}}{k} \tag{9}$$

In circular pipes, the hydraulic diameter, D_h [m], is calculated using the cross-sectional area of the pipe, A_c [m^2], and the perimeter of the pipe, P [m], and given in eq. (7). Calculations regarding the average heat transfer coefficient, h [Wm^{-2}K^{-1}], and Nusselt number are given in eqs. (8) and (9):

$$\mathrm{Re} = \frac{\rho U D_\mathrm{h}}{\mu} \tag{10}$$

The non-dimensional Reynolds number is calculated with the following formula using D_h, velocity U [ms^{-1}], density ρ [kgm^{-3}] and dynamic viscosity μ [kgm^{-1}s^{-1}].

Pressure drops may occur due to the friction in flows occurring in the pipe:

$$\Delta P = \frac{fL\rho U^2}{2D_\mathrm{h}} \tag{11}$$

Pressure drops are indicated with ΔP [Pa]:

$$f = \frac{2D_\mathrm{h}\Delta P}{L\rho U^2} \tag{12}$$

The resulting pressure drops are given in eq. (11) as a function of the friction factor. In this formula, the non-dimensional friction factor f is calculated by eq. (12).

To obtain the advantage of sinusoidal parts, a heat transfer rate comparison is made between the pipe with turbulator and the empty (without turbulator) pipe at equal pumping power. Equal pumping power is given in eq. (13):

$$(\dot{Q}\Delta P)_\mathrm{a} = (\dot{Q}\Delta P)_\mathrm{o} \tag{13}$$

Here, $\dot{Q}$ [m^{3}h^{-1}] shows volumetric flow rate. Then from eq. (13), the relationship between f and Reynolds number can be written:

$$(f\,\mathrm{Re}^3)_\mathrm{a} = (f\,\mathrm{Re}^3)_\mathrm{o} \tag{14}$$

$$PEC = \left.\frac{h_a}{h_o}\right|_{pp} = \left.\frac{Nu_a}{Nu_o}\right|_{pp} = \frac{\dfrac{Nu_a}{Nu_o}}{\left(\dfrac{f_a}{f_o}\right)^{\frac{1}{3}}} \tag{15}$$

The general thermal performance parameter, that is the thermal enhancement factor (PEC) at the same pumping power, is shown as follows using the Nu_a and the friction factor f_a of the pipe with turbulator, and the Nu_o and the friction factor f_o of the plain pipe without turbulator.

Uncertainty analysis

Experimental errors and uncertainties can arise from device selection, device status, device calibration, environment, observation and reading, and test planning. The uncertainty analysis is needed to prove the accuracy of the experiments [23]. Uncertainties in empirically measured quantities can be used in the form of mathematical relationships to calculate the derived quantities considered. Generally, if the output quantity Y can be written as a function of the given input sizes $X_1, X_2, \ldots, X_n$, it is shown as $Y = F(X_1, X_2, \ldots, X_n)$ [24].

The combined uncertainty of the output quantity $U_c(y)$ can be calculated as follows with the standard uncertainty of the input data $u(x_i)$ [25].

$$U_c(y) = \sqrt{\left[\frac{\dfrac{\partial Y}{\partial X_1}}{u(x_1)}\right]^2 + \left[\frac{\dfrac{\partial Y}{\partial X_2}}{u(x_2)}\right]^2 + \ldots + \left[\frac{\dfrac{\partial Y}{\partial X_n}}{u(x_n)}\right]^2} \tag{16}$$

where ∂Y refers to uncertainties related to dependent variables and $x_1, x_2, x_3, \ldots, x_n$ refers to uncertainties related to independent variables.

Experimental uncertainties can result from device selection, calibration, observation, reading, planning, and in some cases environmental errors [26].

The total precision ratio in data readings from the flow meter is ±0.05'dir. In the experimental set-up, the temperatures were measured by using T-type Cu-constantan thermoelements with a diameter of 0.25 mm. The temperature reading accuracy of these thermocouples is around ±0.5 °C. Temperature measurements were made with the connection of thermocouples to the data reading card. The total error rate in the data received from the pressure transducer is at the level of ±0.01. As a result of the error analysis of the power supply, it was estimated that the total error rate in the measurement of electrical power values was at the level of ±0.2%. The uncertainties calculated for Reynolds number, friction factor, f, and Nusselt number are given in tab. 2.

Table 2. Uncertainties of the Reynolds number, *f*, and Nusselt number in percentage

Re	f	Nu
5.85%	4.75%	3.50%

Results and discussion

The studies were examined with the help of the graphics prepared as a result of the data obtained from the experiments. Single-phase flow in the empty pipe and pipes with turbulators were evaluated individually.

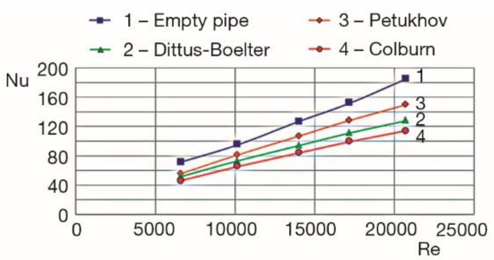

Figure 8. The Nu-Re variation in the empty pipe

The data obtained as a result of the single-phase flow in the empty pipe is shown as a graphic in fig. 8. As can be seen from the graphic, the results obtained are in conformity with the literature. In the light of the data obtained from the experiments, it was determined that Nu = 0.0256 $\text{Re}^{0.8343}\text{Pr}^{1/3}$.

As shown in fig. 8, Nusselt number increases as a result of the increase in the Reynolds number. The Nusselt number calculated as a result of this corresponds to the accepted Colburn, Dittus-Boelter, and Petukhov equations.

– Colburn correlation:

$$\text{Nu} = 0.023\text{Re}^{0.8}\,\text{Pr}^{1/3}, \quad (\text{Re} > 10^4,\, 0.7 \le \text{Pr} \le 160) \tag{17}$$

– Dittus-Boelter correlation:

$$\text{Nu} = 0.023\text{Re}^{0.8}\,\text{Pr}^{n}, \quad (\text{Re} > 10^4,\, 0.7 \le \text{Pr} \le 160) \tag{18}$$

If the fluid flowing through the pipe is heated, *n*, is taken as 0.4, and in the case of cooling the fluid flowing through the pipe, *n*, is taken as 0.3. In this study, since the fluid flowing through the pipe was heated, *n*, was taken as 0.4.

– Petukhov correlation:

$$\text{Nu} = \frac{\dfrac{f}{8}(\text{Re}\,\text{Pr})}{\left[1.07 + 12.7\dfrac{f}{8}\left(\text{Pr}^{\frac{2}{3}} - 1\right)\right]}, \quad (10^4 < \text{Re} < 5\times10^6,\, 0.5 \le \text{Pr} \le 2000) \tag{19}$$

The *f*-Re graph of the data obtained as a result of the single-phase flow in an empty pipe is given in fig. 9. As seen in the graph, there is an inverse proportion between the friction factor *f* and the Reynolds number. While the Reynolds number increases, the friction factor decreases in accordance with the literature.

As seen in fig. 9, the initial values of the friction factor for the empty pipe are higher than the subsequent values. The reason for this is that the pressure drop cannot be detected precisely in low-speed flows.

To prove the accuracy of the experimental set-up, the Blasius equation, which is known in the literature and used for the comparison of smooth empty pipe test data was used [27].

– Blasius equation:

$$f = (0.316)\,\text{Re}^{-0.25} \tag{20}$$

However, considering that the precision value for the Blasius equation is around 25%, such an error is a possible result [28]. As a result of the research, the friction factor was calculated as $f = (7355.2)\text{Re}^{-1.037}$.

Variations of Nu-Re values for turbulators with *R* = 20 mm, 110 mm, and 220 mm radius and the empty pipe are shown graphically in fig. 10.

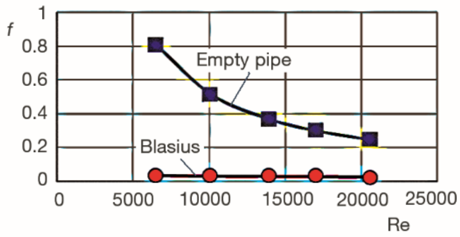

Figure 9. The *f*- Re variation in the empty pipe

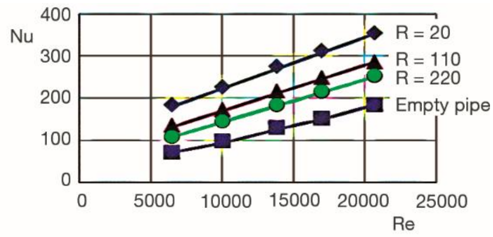

Figure 10. The Nu-Re variation for all measurements

The highest Nusselt number was obtained for the turbulator with the smallest radius. The value of the Nusselt number decreased as the radius increased. Thus, the smallest Nusselt number was reached in a radius of 220 mm compared to 20 mm and 110 mm radii. As a result of the studies carried out, in all turbulent flows, higher Reynolds numbers and accordingly higher Nusselt numbers were achieved compared to the flow in the empty pipe. The *f*-Re variations of all measurements made for R = 20 mm, 110 mm, 220 mm, and empty pipe values are shown graphically in fig. 11. As can be seen from the graphic, the effect of friction increases as the radius value decreases. The highest friction factor was achieved in the turbulator with the lowest radius R = 20 mm. The lowest friction factor in a pipe with turbulator belongs to the test measurement made with turbulators with R = 220 mm. In all experiments performed by placing a turbulator, the friction factor has reached higher values than the empty pipe. In heat transfer improvement studies, it is necessary to take the increase in pressure drop into account as well as the increase in heat transfer. Because passive methods that provide heat transfer increase also cause an increase in pressure drop.

In fig. 12, the variations of the total heat transfer improvement with Reynolds number are presented. In situations above 1, it can be said that the increase in heat transfer is generally more dominant than the increase in pressure drop. Thus, it can be said that the related situation is more beneficial in terms of improving heat transfer. Similarly, in situations below 1, it can be mentioned that the increase in pressure drop is more dominant than the increase in heat transfer. When fig. 12 is examined, it is seen that the inner element with a radius of 20 mm is below 1 in the total heat transfer improvement. This is due to the increase in pressure drop as a result of the 20 mm inner element's blocking the flow too much throughout the

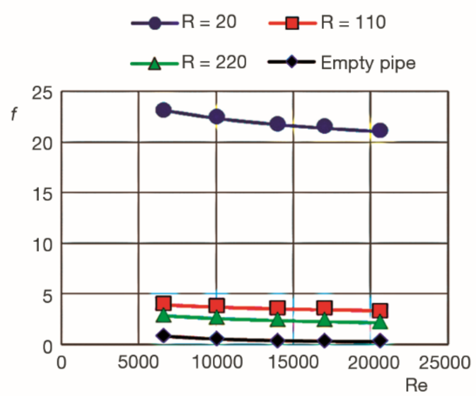

Figure 11. The *f*- Re variation for all measurements

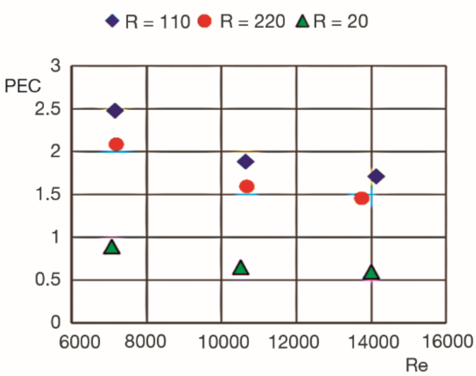

Figure 12. The PEC-Re variation

test area. Although heat transfer increases, the increase in pressure drop is more dominant. Total heat transfer improvement of inner elements with 110 mm and 220 mm radius is above 1. The highest heat transfer improvement was achieved for the inner element with a radius of 110 mm. The data obtained for the thermal enhancement factor are in uniform pumping power and Re number in the range of 6614-20710. The value of the thermal enhancement factor for all in-pipe elements with different radii decreased with increasing Reynolds number. The resistance to fluid-flow caused by the turbulator with a 20 mm radius is more evident than turbulators with a radius of 110 mm and 220 mm. The PEC value increased with the increase in radius value, but in the comparison between the 110 mm and 220 mm radii turbulators, the PEC value was decreased as the radius increased. Here, it turns out that the most ideal turbulator for PEC value is the turbulator of 110 mm radius.

In this study, PEC values as a result of the experiments performed in the range of 6614-20710 Reynolds number were obtained as 0.88, 2.05 and 2.46 for 20 mm, 220 mm, and 110 mm radius turbulators, respectively.

In order to better evaluate the thermal performance of new types of turbulators with different radii, a comparison was made with similar researches in the literature and presented in tab. 3. For this reason, it can be concluded that the new type of turbulators used in this research has a high thermal performance when compared with the other six developed different structures mentioned in the literature. Therefore, the new type of turbulators examined in this research is important in terms of increasing the heat transfer area and thus the heat transfer and being used for application in heat exchangers, industrial type boilers, and heating boilers. Since the turbulators examined in this study will provide advantages in terms of heat transfer, they are recommended to be used in applications.

Table 3. Comparison between the present study and other reported studies

Authors	Enhanced structures	PEC	Re
Present study	wave turbulators	0.88-2.46	6614-20710
Promvonge and Skullong [29]	V-shaped baffle vortex generator	2.14-2.34	4192-25750
Chokphoemphun *et al.* [30]	quadruple counter-twisted tapes	max. 1.33	5300-24000
Hong *et al.* [31]	Multiple twisted tapes	0.88-0.94	5800-19200
Promvonge *et al.* [32]	30° angle-finned tapes	about 1.8	4000-23000
Promvonge [33]	30° V-fins and quadruple counter-twisted tapes	about 1.75	4000-30000
Nakhchi and Esfahani [34]	perforated conical rings	1.24	4000-14000

Conclusions

In this experimental study where the effects of turbulators placed in a pipe where single-phase flow occurs were investigated, experiments were carried out with turbulators with three different radius. As a result of the experiments, the following results were achieved.

As a result of the increase in the Reynolds number, the Nusselt number also increases. This is compatible with Colburn, Dittus-Boelter, and Petukhov equations, accepted in the literature. In experiments, the highest Nusselt number value was obtained in the turbulator with the smallest radius. The value of the Nusselt number decreased as the radius increased.

The order of Nusselt number values according to the radii (for R = 20, 110, and 220 mm) is $Nu_{20} > Nu_{110} > Nu_{220}$. The Nusselt number values obtained from all experiments performed using turbulator are higher than the Nusselt number values obtained from the experiment with an empty pipe. As a result of the experiments, Nusselt number of turbulators with 20 mm, 110 mm, and 220 mm radius compared to the empty pipe were increased by 153.49%, 85.36%, and 52.09%, respectively. When the friction factor occurring in the turbulent flows using turbulator was compared with the friction factor in the empty pipe, it was determined that there were significant increases. The highest friction factor was obtained in experiments with the turbulator with the smallest radius. The friction factor decreased as the radius increased. The order of the values of friction factors according to turbulator radii is $f_{20} > f_{110} > f_{220}$. Considering the friction factors obtained from the experiments, it was determined that the turbulators with a radius of R = 20 mm required the highest pumping power. Considering the friction factor obtained from experiments with the turbulator with a radius of R = 220 mm, it was determined that the lowest pumping power could be obtained by using this turbulator type. The sequence of powers required for pumping based on radii is $R_{20} > R_{110} > R_{220}$. It is seen that the pipe with turbulator with a radius of R = 20 mm is below 1 in the total heat transfer improvement. The total heat transfer improvement of the pipe with turbulator with a radius of R = 110 mm and R = 220 mm is above 1. The highest heat transfer improvement was obtained for the pipe with turbulator with a radius of R = 110 mm. Thermal enhancement factors of 110 mm and 220 mm radius turbulators increased by 179.54% and 132.95%, respectively, compared to 20 mm radius turbulator. Similarly, it was determined that the thermal enhancement factor of the 110 mm radius turbulator increased by 20% compared to the 220 mm radius turbulator.

Nomenclature

f – friction factor
f_o – friction factor of pipe without turbulator
L – test tube length, [m]
Nu – Nusselt number (= hD/k)
Pr – Prandtl number
Q – heat transfer rate, [W]
ΔP – pressure drop, [Pa]
P_i – inlet pressure, [Pa]
P_o – outlet pressure, [Pa]
R – turbulator radius, [mm]
Re – Reynolds number, (= $\rho U D_h/\mu$)
Nu_o – Nusselt number of pipe without turbulator
$U(x_i)$ – input data standard uncertainty
$u_c(y)$ – output quantity combined uncertainty
$x_1, \ldots, x_n$ – uncertainty regarding independent variables
Y – output quantity

Subscripts

a – pipe with turbulator
conv – convection
n – coefficient (0.4 for heating, 0.3 for cooling)
o – straight pipe without turbulator
pp – pumping power
w – wall

References

[1] Vaisi, A., *et al.*, Experimental Investigation of Perforated Twisted Tapes Turbulator on Thermal Performance in Double Pipe Heat Exchangers, *Chemical Engineering and Processing – Proces Intensification*, *154* (2020), Aug., 108028
[2] Vaisi, A., *et al.*, Experimental Investigation of Geometry Effects on the Performance of a Compact Louvered Heat Exchanger, *Applied Thermal Engineering*, *31* (2011), 16, pp. 3337-3346
[3] McDonald, A. G., Magande, H. L., *Introduction to Thermo-Fluids Systems Design*, Wiley Online Library, New York, USA, 012
[4] Shah, R. K., Sekulic, D. P., *Fundamentals of Heat Exchanger Design*, Wiley Online Library, New York, USA, 2003
[5] Fakheri, A., Heat Exchanger Efficiency, *Journal of Heat Transfer, 129* (2007), 9, pp. 1268-1276

[6] Singh, V., *et al.*, Heat Transfer and Fluid Flow Characteristics Of Heat Exchanger Tube with Multiple Twisted Tapes and Solid Rings Inserts, *Chemical Engineering and Processing – Proces Intensification, 102* (2016), Apr., pp. 156-168
[7] Bagherzadeh, S. A., *et al.*, Effects of Magnetic Field on Micro Cross Jet Injection of Dispersed Nanoparticles in a Microchannel, *International Journal of Numerical Methods for Heat and Fluid Flow, 30* (2019), 5, pp. 2683-2704
[8] Li, Z., *et al.*, Operation Analysis, Response and Performance Evaluation of a Pulsating Heat Pipe for Low Temperature Heat Recovery, *Energy Conversion and Management, 222* (2020), Oct., 113230
[9] Li, Z., *et al.*, Pool Boiling Heat Transfer to CuO-H_2O Nanofluid on Finned Surfaces, *International Journal of Heat and Mass Transfer, 156* (2020), Aug., 119780
[10] Khoshvaght-Aliabadi, M., Feizabadi, A., Employing Wavy Structure to Enhance Thermal Efficiency of Spiral-Coil Utilized in Solar Ponds, *Solar Energy, 199* (2020), Mar., pp. 552-569
[11] Kareem, Z. S., *et al.*, Passive Heat Transfer Enhancement Review in Corrugation, *Experimental Thermal and Fluid Science, 68* (2015), Nov., pp. 22-38
[12] Chokphoemphun, S., *et al.*, Heat Transfer Augmentation in a Circular Tube with Winglet Vortex Generators, *Chinese Journal of Chemical Engineering, 23* (2015), 4, pp. 605-614
[13] Yaningsih, I., *et al.*, Thermal Hydraulic Characteristics of Turbulent Single-Phase Flow in an Enhanced Tube Using Louvered Strip Insert with Various Slant Angles, *International Journal of Thermal Sciences, 134* (2018), Dec., pp. 355-362
[14] Yakut, K., Sahin, B., Flow Induced Vibration Analysis of Conical Rings Used for Heat Transfer Enhancement in Heat Exchangers, *Applied Energy, 78* (2004), 3, pp. 273-288
[15] Anvari, A. R., *et al.*, Experimental Research on Heat Transfer of Water in Tubes with Conical Ring Inserts In Transient Regime, *International Communications in Heat and Mass Transfer, 38* (2011), 5, pp. 668-671
[16] Promvonge, P., Eiamsa-ard, S., Heat Transfer Behaviours in a Tube with Combined Conical-Ring and Twisted-Tape Insert, *International Communications in Heat and Mass Transfer, 34* (2007), 7, pp. 849-859
[17] Bhattacharyya, S., *et al.*, Experimental and Numerical Analysis of Forced Convection in a Twisted Tube, *Thermal Science, 23* (2019), 4, pp. 1043-1052
[18] Kapse, A. A., *et al.*, Thermohydraulic Performance Comparison of Compound Inserts for a Turbulent Flow Through a Circular Tube, *Thermal Science, 21* (2017), 3, pp. 1309-1319
[19] Sahel, D., *et al.*, Effect of the Size of Graded Baffles on the Performance of Channel Heat Exchangers, *Thermal Science, 24* (2020), 2A, pp. 767-775
[20] Menni, Y., *et al.*, Heat and Mass Transfer of Oils in Baffled and Finned Ducts, *Thermal Science, 24* (2020), Suppl. 1, pp. S267-S276
[21] Ameur, H., *et al.*, Numerical Investigation of the Performance of Perforated Baffles in a Plate-Fin Heat Exchanger, *Thermal Science*, *25* (2021), 5B, pp. 3629-3641
[22] Chingtuaythong, W., *et al.*, Heat Transfer Characterization in a Tubular Heat Exchanger with V-Shaped Rings, *Applied Thermal Engineering, 110* (2017), Jan., pp. 1164-1171
[23] Ozgener, O., Hepbasli, A., Experimental Performance Analysis of a Solar Assisted Ground-Source Heat Pump Greenhouse Heating Systems, *Energy and Buildings, 37* (2005), 1, pp. 101-110
[24] Afshari, F., *et al.*, Characterization of Lubricating Oil Effects on the Performance of Reciprocating Compressors in Air-Water Heat Pumps, *International Journal of Refrigeration, 74* (2017), Feb., pp. 503-514
[25] Afshari, F., *et al.*, Influence of Refrigerant Properties and Charge Amount on Performance of Reciprocating Compressor in Air Source Heat Pump, *Journal of Energy Engineering, 143* (2017), 1, 04016025
[26] Bakirci, K., *et al.*, Energy Analysis of a Solar-Ground Source Heat Pump System with Vertical Closed-Loop for Heating Applications, *Energy, 36* (2011), 5, pp. 3224-3232
[27] Dogan, M., İgci, A. A., An Experimental Comparison of Delta Winglet And Novel Type Vortex Generators For Heat Transfer Enhancement in a Rectangular Channel and Flow Visualization with Stereoscopic PIV, *International Journal of Heat and Mass Transfer, 164* (2021), Jan., 120592
[28] Abdi, H., Experimental and Theoretical Investigations of the Impact of Turbulators in Horizontal Pipes on Heat Transfer, M. Sc. thesis, Ataturk University, Erzurum, Turkey, 2014, https://tez.yok.gov.tr/UlusalTezMerkezi/tezSorguSonucYeni.jsp
[29] Promvonge, P., Skullong, S., Enhanced Thermal Performance in Tubular Heat Exchanger Contained with V-Shaped Baffles, *Applied Thermal Engineering, 185* (2021), Feb., 116307

[30] Chokphoemphun, S., *et al.*, Thermal Performance of Tubular Heat Exchanger with Multiple Twisted-Tape Inserts, *Chinese Journal of Chemical Engineering, 23* (2015), 5, pp. 755-762
[31] Hong, Y., *et al.*, Turbulent Thermal, Fluid Flow and Thermodynamic Characteristics in a Plain Tube Fitted with Overlapped Multiple Twisted Tapes, *International Journal of Heat and Mass Transfer, 115* (2017) Part B, Dec., pp. 551-565
[32] Promvonge, P., *et al.*, Heat Transfer in Square Duct Fitted Diagonally with Angle-Finned Tape-Part 1: Experimental study, *International Communications in Heat and Mass Transfer, 39* (2012), 5, pp. 617-624
[33] Promvonge, P., Thermal Performance in Square-Duct Heat Exchanger with Quadruple V-Finned Twisted Tapes, *Applied Thermal Engineering, 91* (2015), 5, pp. 298-307
[34] Nakhchi, M. E., Esfahani, J. A., Numerical Investigation of Different Geometrical Parameters of Perforated Conical Rings on Flow Structure and Heat Transfer in Heat Exchangers, *Applied Thermal Engineering, 156* (2019), June, pp. 494-505

Paper submitted: February 6, 2021
Paper revised: April 6, 2021
Paper accepted: April 9, 2021